

ACCEPTED VERSION

Lawley, Evertje Frederika; Lewis, Megan Mary; Ostendorf, Bertram Franz
[Environmental zonation across the Australian arid region based on long-term vegetation dynamics](#), *Journal of Arid Environments*, 2011; 75(6):576-585

Copyright © 2011 Elsevier Ltd.

PERMISSIONS

<http://www.elsevier.com/wps/find/authorsview.authors/rights>

[The author retains] the right to post a revised personal version of the text of the final journal article (to reflect changes made in the peer review process) on your personal or institutional website or server for scholarly purposes, incorporating the complete citation and with a link to the Digital Object Identifier (DOI) of the article.

15th November, 2011

<http://hdl.handle.net/2440/66560>

Environmental zonation across the Australian arid region based on long term vegetation dynamics

Erika F. Lawley^a, Megan M. Lewis, Bertram Ostendorf

School of Earth & Environmental Sciences, The University of Adelaide, Adelaide, SA 5005, Australia

^a *Corresponding author: E.F. Lawley, School of Earth and Environmental Sciences, The University of Adelaide, South Australia 5005, Australia. Ph: +61 8 8303 6571, Fax: +61 8 8303 6717, e-mail: evertje.lawley@adelaide.edu.au*

1. Introduction

Classification of arid landscapes into units with characteristic climate, landforms, soils and vegetation provides a foundation for survey, conservation and management.

Stratification of the landscape has been practiced worldwide and classifications are refined or updated as more information and data become available (Blasi et al., 2000; Cihlar et al., 1996; Jongman et al., 2006; Mucher et al., 2010; Townshend et al., 1991).

In Australia, as in many parts of the world, an integrated landscape approach to environmental stratification has been adopted. The Interim Biogeographical Regionalization for Australia (IBRA) defines 85 biogeographic regions, 39 of which fall wholly or mostly in the arid zone. The regions are defined on the basis of climate, geology, landform, vegetation and fauna (Thackway and Cresswell, 1997). In highly modified landscapes, such as those of Europe, ecoregions are similarly defined, although in the absence of natural vegetation, potential natural vegetation is inferred (Pesch et al., 2009).

27 Fundamental to the integrated approach is the assumption that climate, geology and
28 geomorphology interact over time to produce characteristic landscape patterns and
29 influence the distribution of soil and vegetation associations, which in turn influence
30 faunal assemblages. Consequently there are associations of these environmental
31 components and landscape can be classified and mapped into units with characteristic
32 and recurring patterns and a degree of internal homogeneity.

33

34 In Australia this approach traces its origins back to the integrated land system survey
35 embodied in the CSIRO Land Use Series (Christian and Stewart, 1953), later developed
36 by Laut et al. (1977) for Environments of South Australia. Environmental units are
37 defined by recurring landscape patterns interpreted from broad scale imagery (initially
38 aerial photography, now more commonly multispectral satellite imagery), drawing on
39 field surveys, broad scale biophysical data and expert knowledge to characterise the
40 mapping units.

41

42 This represents, however, a static view of the environment, based on associations of
43 climate, geomorphology, soil and vegetation, and does not necessarily account for the
44 dynamics and function of the landscape. Australian arid landscapes in particular are
45 highly dynamic and far from static, although differences in function may not be readily
46 discerned on the ground, and are expressed over long periods of time.

47

48 Long-term sequences of satellite imagery from sensors such as NOAA AVHRR and
49 MODIS now provide a means of observing the dynamics of landscapes over broad areas
50 and long periods, and hence can provide an understanding of the function as well as

51 distribution of landscape types. Actively growing vegetation within landscapes can be
52 detected using the Normalised Difference Vegetation Index (NDVI), which calculates
53 the difference in reflectance between the near-infrared and visible red bands divided by
54 the sum of these two bands (Tucker, 1979). NDVI represents the chlorophyll abundance
55 and energy absorption of the leaves (Myneni et al., 1995) and has been correlated with
56 leaf area index, vegetation cover and biomass. In arid landscapes this is influenced by
57 vegetation response to rainfall and by such factors as soil moisture absorption and
58 holding capacity and vegetation type which itself may change over time as a result of
59 the stochastic events of fire, flood or grazing.

60

61 Satellite imagery has been used to investigate temporal patterns in NDVI ever since it
62 became available in the 1980's. Initially based only on few dates within a single year to
63 stratify vegetation using a climatic gradient (Norwine and Greigor, 1983), later studies
64 expanded to multiple dates per year and inter-annual comparisons. Investigations of
65 landscape dynamics have included studies of mechanisms affecting primary production
66 across modified landscapes such as those in Brazil (Barbosa et al., 2006) and
67 monitoring of land use change (Al-Bakri and Taylor, 2003; Neigh et al., 2008; Turcotte
68 et al., 1993; Weiss et al., 2004). Using time-sequences of NDVI these studies generally
69 sought to identify or detect a change in particular landscape features.

70

71 The current study, on the other hand, seeks to understand the variability inherent in the
72 landscape. It presents an analysis of the patterns of spatial and temporal variation of
73 vegetative growth across the Australian arid zone, as revealed by a 25 year sequence of
74 NOAA AVHRR bi-monthly NDVI composites. Our aim is to understand the dynamics

75 and functional response of vegetation in the region and use this to inform and
76 potentially improve the IBRA of the Australian arid zone. Specifically we seek to
77 identify the underlying factors influencing patterns of arid vegetation growth and map
78 the distribution of regions with similar response. This new classification is compared
79 with the IBRA and used to evaluate the composition and boundaries of IBRA regions:
80 our analysis sought to determine whether the IBRA classes are consistent with long-
81 term evidence of vegetation response.

82 **2. Methods**

83 *2.1 Study area*

84 The limits of an arid zone are not rigid and can be defined according to the purpose of
85 an investigation. The global agro-climatic classification for instance focuses on climate
86 constraints on crop growth, and defines as arid the Australian region too dry to support
87 field crops (Hutchinson et al., 1992; Hutchinson et al., 2005). The modified Köppen
88 classification of world climates indicates a larger arid zone in Australia, comprising two
89 categories, desert and grassland, where evaporation exceeds precipitation, defined by
90 maximum, minimum and mean temperature, and mean rainfall records. (BOM ;
91 Hutchinson, 1995; Stern et al., 2000). This larger arid definition includes, mainly at its
92 margins, some dryland cultivated areas.

93 To include the maximum area of dry land natural vegetation cover, the current study
94 used the modified Köppen definition of the arid zone. Recognising that cultivated
95 vegetation response within this zone may confound the analysis of natural vegetation
96 response, cultivated areas as indicated on the Australian Land Use Map (ALUM, 2000)

97 were masked from the study area, resulting in the arid zone outline used for the current
98 study (Fig. 1).

99 *Insert Figure 1 approx. here*

100 The approximately 5,250,000 km² area contains a great diversity of land types and
101 vegetation, including tussock and hummock grasslands, chenopod shrublands, tall open
102 and closed shrublands and low woodlands both open and closed, with herbaceous,
103 grassland or shrub understorey. Mean annual rainfall ranges up to 400 mm in the north
104 and 250 mm in the south.

105 **2.2 NDVI data**

106 This study used a series of 600 NDVI images which were derived from data collected
107 daily from 1982 to 2006, by the Advanced Very High Resolution Radiometer (AVHRR)
108 aboard the United States National Oceanographic and Atmospheric Administration
109 (NOAA) polar orbiting satellite. The satellite data was corrected for atmospheric effects
110 and cloud cover, calculated at maximum reflectance over half month intervals, and
111 resampled from the original 1.1 km to 8 km spatial resolution, by the University of
112 Maryland Global Land Cover Facility (GLCF) for the Global Inventory Modeling and
113 Mapping Studies (GIMMS) (Pinzon et al., 2005; Tucker et al., 2005). The files had been
114 converted from native binary to GeoTIFF format. NDVI values had been scaled to
115 values ranging from -10000 to 10000, water pixels had been assigned the value of -
116 10000, and masked pixels -5000. This scaling was maintained for the current study
117 because absolute NDVI values were not required. The NDVI range of -1 to 1 can be
118 recovered, if required, using the formula: $NDVI = \text{float}(\text{raw}/10000)$ (GLCF 2008). The

119 data were obtained as continental files, Albers projection, and were for this study
120 reprojected to South Australian Lambers Conformal Conic.

121

122 A visual inspection revealed sensor and mosaicking artifacts in several images. These
123 images were retained within the data stack, noting the image dates, on the assumption
124 that if the artifacts are the source of significant variation, it would be revealed by the
125 principal component analysis, and if not, the anomaly would be consigned to noise.

126 *2.3 Principal component analysis*

127 In order to examine the modes of variation within the 25-year NDVI sequence, principal
128 component analysis (PCA) was applied to the data set. This is a linear transformation of
129 correlated variables into uncorrelated variables retaining the same number of variables
130 but eliminating redundancy. The transformed variables are independent and ordered
131 from the first component representing the maximum variance within the data set, down
132 to the subsequent components representing progressively less variance. It is a useful
133 technique to reveal the areas of greatest spatial and/or temporal variability within a
134 landscape based on the distribution of eigenvalues and explained variance and by
135 linking the interpretation of the principal components to the geography of the area under
136 investigation (Eastman and Fulk, 1993; Roberts, 1994).

137

138 The orthogonal character of unstandardised PCA (uPCA), which uses the covariance
139 matrix, imposes constraint (Eastman and Fulk, 1993), and relaxing this constraint by
140 using the correlation matrix (standardised PCA) is claimed to give better temporal or
141 spatial representation of the underlying processes (Fung and Ledrew, 1987; Hall-Beyer,

142 2003). While such improvement was apparent in shorter time series of, for example, 12
143 images (Eklundh and Singh, 1993) and standardisation has also been used to improve
144 signal-to-noise ratio, for the current study no advantage appeared to be gained by
145 standardising the analysis. Standardisation may be judicious when using data from
146 several disparate geographical areas (Weiss et al., 2004) but this is not the case for the
147 current study. Inspection of the first PCs while preparing the data revealed little
148 difference between the two methods, apart from inversion of the resultant PC scores.
149 Inversion is of no consequence, as polarisation is a result of the options chosen by the
150 image analysis software in generating the PCs and does not affect the magnitude or
151 meaning of the results. The covariance matrix (uPCA) was therefore used in the study
152 and all bands were included to avoid loss of meaningful information.

153

154 PCA transformed the data into 600 PCs. Eigenvalues were inspected to detect the
155 percentage of variation explained by each PC and eigenvector loadings for each PC
156 were plotted against the image dates. The PC image patterns and associated plots were
157 scrutinized together with relevant climate records to analyse the factors that account for
158 the variation in the multidimensional data space. To aid understanding a colour
159 composite was created of the first 2 PCs. The latest available revision of IBRA, v6.1,
160 was used as overlay to indicate locations and to visually detect correlation between the
161 colour composite patterns and IBRA regions.

162 ***2.4 Classification***

163 PCA reduced the 600 NDVI images to a small number of main components. Of these
164 the first 14 components, representing 85% of the variance in the data, were used as a

165 basis for unsupervised classification. This selection incorporated as much meaningful
166 variability as possible, including PCs representing broad scale as well as localized
167 events, but excluding PCs representing less than 0.5% of variability and potentially
168 representing sensor artifacts and noise. The PCs were used in unstandardised form,
169 hence were weighted in their relative contribution to the classification. Iso-classification
170 using the selected PCs classified image pixels on the basis of similarity of PC profile,
171 with the resultant classification image showing the distribution of classes across the
172 landscape. The number of classes in which to cluster the data was decided by trial,
173 aiming to approximate the number of large IBRA regions within the arid zone. The
174 factors separating the classes were examined through plots of class PC scores and the
175 classes characterized by extracting, out of the original data stack, mean NDVI time
176 traces for each class. The relationship between classes and the IBRA stratification was
177 investigated using GIS analysis.

178 **3. Results**

179 *3.1 Factors in vegetation temporal response*

180 PCA of the 600 image series of the Australian non-cultivated arid zone resulted in 600
181 principal components and their associated matrices. The greatest source of variation in
182 the data (65.05%) was captured by PC1 (Table 1), which clearly represents the
183 geographic distribution of the sum total of NDVI for each pixel, as shown in the PC1
184 image, where white indicates low total vegetation grading to black for high vegetation
185 response (Fig. 2).

186

187 *Insert Table 1 approx. here*

188

189 Geographically the highest aggregate vegetation occurred towards the tropical and
190 subtropical margins of the arid north and north-east, and in the south and south-east
191 where the arid zone borders on temperate areas, as evidenced in the woodlands of
192 Western Australia and South Australia's Conservation Parks. Floodplains of the major
193 inland watercourses in Queensland also showed high aggregate NDVI. Lowest
194 vegetation aggregate was evident in the South Australian Stony Plains and Simpson and
195 Strzeleckie Dunefields and the Channel Country of Queensland (Fig. 1). This low total
196 vegetation was noticeably less pronounced across the Great Victoria Desert and the
197 deserts of Western Australia, areas with similarly low rainfall (mean <250mm pa). Salt
198 lakes, as one would expect, show virtually no aggregated vegetation response in the
199 PC1 image.

200

201 *Insert Figure 2 approx. here*

202

203 *Insert Figure 3 approx. here*

204

205 The associated plot of band loadings for PC 1 revealed a weak tendency towards
206 seasonality. In some, but not all years, total of actively growing vegetation appears
207 lowest around November and highest during the Austral autumn and winter, March to
208 August (Fig. 3).

209

210 The second greatest source of variation, PC 2, captured 7.15% of the variation in the
211 NDVI image sequence. The eigenvector plot shows a clear seasonal contrast with high
212 positive band loadings in October/November and contrasting large negative loadings in

213 March (Fig. 3). Geographically, this component shows the contrast between the
214 extremes of the northern summer rain influenced (Smith et al., 2008) and southern
215 winter rain influenced (Feng et al., 2010) arid zone. These extremes contrast with the
216 lack of strong seasonal response in the centre of Australia (PC 2 in Fig. 2).

217

218 A colour composite illustrates how the two main patterns of variance, that is the
219 aggregate of PC 1 and the seasonality of PC 2, interact (Fig. 4). Cumulatively these two
220 components explain 72.2% of the variance in the data. Dark green in the north shows
221 the main vegetation growth occurs in summer and is overall high. Bright green, mainly
222 in the south, indicates winter growth and high overall greenness, but some darker green
223 shading in the southern region indicates summer growth, consistent with summer green-
224 up characteristic for the native *Eucalyptus* mallee tree areas in Western Australia and
225 South Australia. The dark red areas in the north have overall moderate to low vegetation
226 total with strong summer bias. The centre of the arid zone is not affected by seasonality
227 and has low aggregate vegetation. Some clear contrasts are visible in particular in the
228 north between the Mitchell Grass Downs, with low total vegetation contribution, and
229 adjacent regions with a higher vegetation aggregate, such as the Mount Isa Inlier (Fig.
230 4).

231

232 *Insert Figure 4 approx. here*

233

234 PC 3 explained 2.97% of the remaining variance, showing an irregular east-summer
235 versus west-winter growth contrast (PC 3 in Fig. 2) apparently perturbed by erratically
236 occurring climatic events as shown in the eigenvector plot (Fig. 3). The south west of

237 the arid zone tends to receive winter rain (Feng et al., 2010). Although greening in the
238 east generally occurs in summer, the inland rivers that carry floodwaters from northern
239 rain events through the very arid Channel country, generally do not receive floodwaters
240 until April resulting in the rivers' contrasting appearance (PC 3 in Fig. 2). An
241 exceptionally high loading in July 1990 followed widespread flooding in eastern
242 Australia (Fig. 3). These floods, known as the Charleville, Nyngan Great Floods, at
243 their peak inundated more than one million square kilometres of Queensland and New
244 South Wales, an area larger than all of Germany. In a concurrent but separate event
245 Victoria also was affected by severe flooding (GeoscienceAustralia, 2007). Such
246 periodic rainfall events may cause the otherwise seasonal pattern to become
247 intermittent.

248

249 PC 4 captured 2.1% of the remaining variance in the data. Its plot shows no consistent
250 seasonality but for 2006 its eigenvector loadings are more extreme than any other
251 during the 1982 -2006 period (Fig. 3). This variation in the data appears to be linked to
252 the major rainfall event in connection with cyclone Larry, which struck north eastern
253 Queensland in March 2006. Widespread flooding caused strong vegetation growth. The
254 geographical location of this is clearly evident in NE QLD (PC 4 in Fig. 2).

255

256 Further components explained ever smaller proportions of variance. In time series PCA,
257 as in multispectral PCA, later components, though representing a low proportion of total
258 dataset variance, may represent informational variance for small regions (Hall-Beyer,
259 2003), or significant one-off events. Component 5, for instance, shows a strong seasonal
260 response in the eigenvector plot with extremes in January contrasting with those in June

261 (Fig. 3). The PC image shows clear contrast between various regions (PC 5 in Fig. 2), it
262 becomes however increasingly difficult in the successive PCs to determine the source of
263 variation in vegetation temporal response in each of the contrasting areas.

264

265 The first 14 components captured over 85% of the variation within the total data, as
266 revealed in mean eigenvalues (Table 1). Although components from PC 7 to PC 14
267 explained a very small percentage of the remaining variation, from 1% incrementally
268 down to 0.5 %, they are likely to hold information of some significance because of the
269 very large geographic and temporal extent of the dataset. From PC 20 onwards some
270 PCs showed evidence of sensor artifacts and noise.

271 ***3.2 Classification of vegetation temporal response***

272 The geographic distribution of classes resulting from the unsupervised classification is
273 shown in Fig. 5, together with a three dimensional view of the class PC scores in
274 relation to the dominant factors derived from the PC analysis. The classes are ranked
275 and numbered by the value of the mean scores of PC 1, the greatest source of variation
276 between classes.

277

278 As expected from the PCA, the dominant factor separating the classes is total vegetation
279 growth, with lesser separation according to seasonality of growth, both between north
280 and south and to a less well defined degree between east and west (Fig. 5 b). Classes 1
281 and 24 form the extremes of the high-low vegetation growth continuum (PC 1). Classes
282 2, 4 and 8 are positioned opposite 1, 3 and 5 illustrating the extremes of the north-south

283 seasonal contrast (PC 2), and classes 10, 14 and 18 opposing 5, 7 and 15 show the
284 extremes of the east-west contrast (PC 3).

285

286 *Insert Figure 5 approx. here*

287

288 Mean NDVI temporal traces for the dominant classes indicate how NDVI varies over 25
289 years (Fig. 6). Class 1 has high vegetation response in winter and spring.

290 Geographically it dominates the southwest regions in Western Australia, the
291 conservation parks in the Murray Darling Depression of South Australia and parts of the
292 Cobar Peneplain in New South Wales and it occurs in the Mulga Lands of Queensland
293 (Fig. 1). These areas all have mallee (*Eucalyptus* sp.) vegetation cover in common and
294 are similar to class 3, which occurs generally to the north west of class 1 and shows the
295 same NDVI signature, though at a lower magnitude (Fig. 6). Class 5, occurring in the
296 arid non-cultivated part of the Riverina district, also shows extreme amplitude and
297 fluctuation, and spring growth. The NDVI of this class is likely influenced by rainfall
298 response of the saltbush plains as well as riparian response along the rivers and lakes
299 some of which are fed by rain falling in the temperate zone to the east (Gov-NSW,
300 2002).

301

302 Classes 2, 4, 8 and 9 also show high NDVI and pronounced seasonality of vegetation
303 growth. Their temporal signatures are quite similar with onset of growth often
304 coinciding, although class 2 has greater magnitude, with peaks tending to persist longer
305 than class 4. Class 8 has the lower vegetation response of these, with sharp narrow
306 peaks followed by rapid decline. Geographically these classes occur in the north of the

307 arid zone. For these classes vegetation appears at its lowest from October to December
308 and increases sharply from December onwards, high peaks generally occurring in
309 March.

310

311 By contrast a large part of the landscape showed a fairly uniform response, especially in
312 the most arid part of the arid zone. Classes 21, 22 and 23 are characterised by very low
313 vegetation response with very little seasonality, as indicated by the temporal NDVI plot
314 (Fig. 6). These classes have almost identical temporal signatures, differing from each
315 other only in magnitude. The shape of the NDVI signatures is quite erratic, with one
316 peak in July in each 1983, 88, 89 and 90, but in other years several peaks occur at
317 different times. These classes dominate the north east of South Australia and the south
318 west of Queensland (Fig. 5), which is a sparsely vegetated area, traditionally grazed by
319 cattle. Class 24 shows lowest NDVI, representing the usually dry salt lakes that are a
320 dominant feature in many regions of the Australian arid zone (Fig. 5 a).

321

322 Class 7, located at the eastern margins of the arid zone in Queensland and New South
323 Wales, shows high NDVI levels. Class 15 shows a similar pattern to class 7, with onset
324 of peaks coinciding, but peaks are of different magnitude, with one or the other
325 exceeding at different instances. Class 15 in the eastern region and to a lesser extent
326 class 19 in the western (NT) region of the Mitchell Grass Down shows in some years
327 extremely sharp increases in vegetation growth between December and March. This is
328 when wet season rains activate the Mitchell Grass tussocks (*Astrebla* spp.) and inter-
329 tussock ephemeral herbs and annual grasses (Fisher et al., 2002). Class 19 peaks are
330 generally of lesser amplitude than those of class 15 (Fig. 6).

331

332 *Insert Figure 6 approx. here*

333

334 Classes 17, 18 and 20 dominate the deserts of Western and South Australia. The eastern
335 Nullarbor responded similarly to the Great Victoria Desert to the north of it, but the
336 western and southern parts of the Nullarbor are uniquely identified as class 14 with the
337 south and west margins revealed as class 3 and 4, identified with *Eucalyptus* (mallee)
338 woodland. The non-seasonal arid Nullarbor Plain carries chenopod shrubs with low
339 open woodland at the peripheries (FloraBase, 2009)

340

341 Class 10 occurs mainly in the Carnarvon, and western Murchison and Pilbara area of
342 Western Australia. The NDVI signature for class 10 shows regular high winter
343 vegetation response. Similarity in response was revealed between the eastern
344 Pilbara/north west Great Sandy Desert area and the Central Ranges area, which is
345 located across the South Australian border; at least part of each region was categorized
346 as class 13. The Pilbara features the Hammersley Ranges which are similar to the
347 Central Ranges, however the north western edge of the Great Sandy Desert is a flat
348 monsoonal influenced landscape, arid tropical with summer rain (FloraBase, 2009).
349 Further exploration revealed that the classes 13, 16 and 20 show great similarity in
350 vegetation fluctuation and amplitude (Fig. 6), are characterized by low vegetation
351 response, and appear to be part of the desert continuum reaching north east- south west
352 across the Great Sandy Desert. This underlines the observation that traditional
353 stratification is not able to display the boundary gradations picked up by the NDVI
354 response.

355 ***3.3 Relationship between classification and IBRA***

356

357 The relationship between IBRA regions and classes is illustrated in a matrix which
358 shows the percentage contribution made by the classes to each IBRA region (Fig. 7). In
359 some instances a very strong relationship exists between IBRA region and class. The
360 Riverina IBRA, for instance, is dominated by single class 5 (81%), with minor
361 contributions from related classes, mainly 3, 6 and 11, that have similar NDVI response.
362 Likewise the Finke region is dominated by class 16 (71%) with minor contribution from
363 class 21 (18%). At the other extreme, some IBRA regions are made up of numerous
364 classes of quite diverse NDVI time traces, indicating that these regions contain
365 considerable variability of vegetation response. The Mulga Lands region for instance
366 consists of classes 3, 7, 13, 16 and 21.

367

368 In some instances the classes have distinct boundaries and close correspondence to the
369 IBRA. For example class 12 has sharply defined borders which closely match the
370 northern part of the Mitchell Grass Downs IBRA region, where contrasting soils and
371 vegetation types are juxtaposed. The NDVI temporal analysis confirms that these
372 adjoining land systems have quite different temporal vegetation responses and that the
373 boundary between them is indeed quite distinct. In many areas gradients occur where
374 there is a continuum of classes that show a transition of vegetation temporal response
375 but where the IBRA regionalization suggests distinct boundaries, such as the transition
376 between the Coolgardie and the Murchison regions in Western Australia (class 1, 3 and
377 6).

378

379 *Insert Table 2 approx. here*

380

381 Some IBRA regions comprise several classes, which although showing some similarity
382 in NDVI plot, behave quite differently over time. For instance of the three classes that
383 dominate the Gibson Desert, class 20 shows moderate amplitude and an irregular
384 pattern. Class 16 shows extreme peaks in NDVI, usually in winter, in 1982, 1983 and
385 from 1988 to 1991. Class 18 on the other hand shows such peaks from 1992 to 2006.

386

387 It is clear that the designated large desert IBRA regions are not as internally
388 homogenous as one might expect of low rainfall sparsely vegetated areas. Factors of
389 erratic rainfall and unpredictable wildfires influence the vegetation response, which
390 cannot be seen in the traditional stratification, but appears borne out by the NDVI time
391 traces of the relevant classes in this study.

392 **4. Conclusions**

393 The Australian arid zone is an extremely large region with mean rainfall below 400 mm
394 in the north and 250 mm in the south, but which contains a great diversity of land types
395 and vegetation responses. The analysis in this paper has identified the major patterns of
396 vegetation growth response throughout this region. The dominant factors are variation
397 in a) total vegetation growth over long periods; b) seasonality of vegetation growth with
398 contrasts between summer and winter, autumn and spring; c) magnitude of seasonal
399 variability in growth with contrast between high and very little variation; and d)
400 regularity of variation in growth. In addition to these dominant factors, around 15% of
401 the variation in NDVI response, over the 25 year sequence analysed, resulted from

402 episodic vegetation growth of limited spatial extent and duration, emphasising the
403 considerable unpredictability of rainfall and vegetation growth in the Australian arid
404 zone.

405

406 Using NDVI data that accounted for 85% of the variation in long-term vegetation
407 growth, the Australian arid zone has been classified into 24 classes. These classes are
408 based on similarity and differences in the temporal vegetation growth response
409 described above. This classification considerably adds to our understanding of
410 Australian arid vegetation dynamics and its driving forces. The NDVI temporal
411 classification is based on inherent vegetation change and variation over 25 years of bi-
412 monthly, spatially comprehensive observations of the continent, an approach quite
413 different from the criteria used to delineate the IBRA classes. The classification
414 provides new information about vegetation and landscape function: cycles and pulses or
415 episodes of vegetation growth, the relative magnitude of primary production and
416 standing biomass, and the distribution of regions of similar functional response.

417

418 This information can be used to enhance the current IBRA regionalisation and add a
419 new dimension to definition and characterisation of the regions. It provides new
420 information about the temporal dynamics of vegetation response in the IBRA regions,
421 substantially adding to their current characterization in terms of climate, geology,
422 geomorphology, vegetation composition and fauna. It also provides an independent and
423 objective basis for re-evaluation of the IBRA regions and sub-regions. It highlights
424 areas where IBRA vegetation response is highly variable, and may provide a basis for

425 sub-regionalisation, where environmental boundaries between regions may be
426 questioned or further explored.
427
428 The study also demonstrates a methodology that has wider potential for classification of
429 broad regional landscapes. Whereas traditional approaches to mapping natural
430 environments have relied on interpretation of landscape associations and patterns in
431 photography or satellite imagery, using field survey to characterize the mapping units,
432 our classification is based on the response of vegetation recorded over long periods of
433 time. Regions with similar long-term vegetation dynamics are aggregated, providing a
434 functional basis for landscape stratification. The resultant classes provide a new and
435 valuable basis for ecological survey, biodiversity conservation and environmental
436 management: each unit has a unique association of climate, topography, soil and
437 vegetation, but also a distinctive history and temporal pattern of vegetation response.
438 The growing global archive and ready availability of long-term sequences of NDVI
439 imagery, at resolutions suitable for regional analysis, make this a valuable resource for
440 environmental characterization.

441 **References**

- 442 Al-Bakri, J.T., Taylor, J.C., 2003. Application of NOAA AVHRR for monitoring vegetation
443 conditions and biomass in Jordan. *Journal of Arid Environments*, 54, 579-593.
444 ALUM, 2000. Australian Land Use Map.
445 http://adl.brs.gov.au/findit/metadata_files/pa_luav3r9eg_00112a00.xml.
446 Barbosa, H.A., Huete, A.R., Baethgen, W.E., 2006. A 20-year study of NDVI variability
447 over the Northeast Region of Brazil. *Journal of Arid Environments*, 67, 288-307.
448 Blasi, C., Carranza, M.L., Frondoni, R., Rosati, L., 2000. Ecosystem Classification and
449 Mapping: A Proposal for Italian Landscapes. *Applied Vegetation Science*, 3, 233-
450 242.
451 BOM Australian Bureau of Meteorology. <http://www.bom.gov.au/>.

452 Christian, C.S., Stewart, G.A., 1953. General report on survey of Katherine-Darwin
453 region, 1946. *Land Research Series No. 1*, CSIRO Melbourne Australia.

454 Cihlar, J., Ly, H., Xiao, Q., 1996. Land cover classification with AVHRR multichannel
455 composites in northern environments. *Remote Sensing of Environment*, 58, 36-
456 51.

457 Eastman, J.R., Fulk, M., 1993. Long Sequence Time-Series Evaluation Using
458 Standardized Principal Components. *Photogrammetric Engineering and Remote
459 Sensing*, 59, 991-996.

460 Eklundh, L., Singh, A., 1993. A comparative analysis of standardised and
461 unstandardised Principal Components Analysis in remote sensing. *International
462 Journal of Remote Sensing*, 14, 1359 - 1370.

463 Feng, J., Li, J.P., Li, Y., 2010. A Monsoon-Like Southwest Australian Circulation and Its
464 Relation with Rainfall in Southwest Western Australia. *Journal of Climate*, 23,
465 1334-1353.

466 Fisher, A., Baker, B., Woinarski, J., 2002. Mitchell Grass Downs (Northern Territory)
467 bioregional case study. Darwin, Parks and Wildlife Commission of the Northern
468 Territory, Darwin
469 <http://www.anra.gov.au/topics/vegetation/assessment/index.html#biodiversity>

470 FloraBase, 2009. The Western Australian Flora.
471 <http://florabase.calm.wa.gov.au/help/ibra/#map>.

472 Fung, T., Ledrew, E., 1987. Application of Principal Components-Analysis to Change
473 Detection. *Photogrammetric Engineering and Remote Sensing*, 53, 1649-1658.

474 GeoscienceAustralia, 2007. Major historic floods.
475 <http://www.ga.gov.au/hazards/flood/historic.jsp>.

476 Gov-NSW, 2002. The bioregions of New South Wales - their biodiversity, conservation
477 and history - chapter 8.
478 www.environment.nsw.gov.au/resources/nature/riverina.pdf.

479 Hall-Beyer, M., 2003. Comparison of single-year and multiyear NDVI time series
480 principal components in cold temperate biomes. *Ieee Transactions on
481 Geoscience and Remote Sensing*, 41, 2568-2574.

482 Hutchinson, M.F., Nix, H.A., McMahon, J.P., 1992. Climate constraints on cropping
483 systems. In Pearson, C.J. (Ed.) *Field Crop Ecosystems: Ecosystems of the World.
484 Vol 18*. Amsterdam, Elsevier Science Publishers.

485 Hutchinson, M.F., 1995. Interpolating mean rainfall using thin-plate smoothing splines.
486 *International Journal of Geographical Information Systems*, 9, 385-403.

487 Hutchinson, M.F., McIntyre, S., Hobbs, R.J., Stein, J.L., Garnett, S., Kinloch, J., 2005.
488 Integrating a global agro-climatic classification with bioregional boundaries in
489 Australia. *Global Ecology and Biogeography*, 14, 197-212.

490 Jongman, R., Bunce, R., Metzger, M., Mücher, C., Howard, D., Mateus, V., 2006.
491 Objectives and Applications of a Statistical Environmental Stratification of
492 Europe. *Landscape Ecology*, 21, 409-419.

493 Laut, P., Keig, G., Lazarides, M., Löffler, E., Margules, C., Scott, R., Sullivan, M.E., 1977.
494 *Environments of South Australia - Province 8, Northern Arid*, Commonwealth
495 Scientific and Industrial Research Organisation, Canberra.

496 Mucher, C.A., Klijn, J.A., Wascher, D.M., Schaminee, J.H.J., 2010. A new European
497 Landscape Classification (LANMAP): A transparent, flexible and user-oriented
498 methodology to distinguish landscapes. *Ecological Indicators*, 10, 87-103.

499 Myneni, R.B., Hall, F.G., Sellers, P.J., Marshak, A.L., 1995. The interpretation of spectral
500 vegetation indexes. *Geoscience and Remote Sensing, IEEE Transactions on*, 33,
501 481-486.

502 Neigh, C.S.R., Tucker, C.J., Townshend, J.R.G., 2008. North American vegetation
503 dynamics observed with multi-resolution satellite data. *Remote Sensing of
504 Environment*, 112, 1749-1772.

505 Norwine, J., Greigor, D.H., 1983. Vegetation Classification Based on Advanced Very
506 High-Resolution Radiometer (Avhrr) Satellite Imagery. *Remote Sensing of
507 Environment*, 13, 69-87.

508 Pesch, R., Schmidt, G., Schroeder, W., Weustermann, I., 2009. Application of CART in
509 ecological landscape mapping: Two case studies. *Ecological Indicators*, In Press,
510 Corrected Proof.

511 Pinzon, J., Brown, M.E., Tucker, C.J., 2005. Satellite time series correction of orbital
512 drift artifacts using empirical mode decomposition. In Huang, N. (Ed.) *Hilbert-
513 Huang Transform: Introduction and Applications*. 167-186.

514 Roberts, M., 1994. Component Analysis for the interpretation of Time Series NDVI
515 Imagery. *ASPRS/ACSM*.

516 Smith, I.N., Wilson, L., Suppiah, R., 2008. Characteristics of the northern Australian
517 rainy season. *Journal of Climate*, 21, 4298-4311.

518 Stern, H., de Hoedt, G., Ernst, J., 2000. Objective classification of Australian climates.
519 *Australian Meteorological Magazine*, 49, 87-96.

520 Townshend, J., Justice, C., Li, W., Gurney, C., McManus, J., 1991. Gobar Land Cover
521 Classification by Remote-Sensing - Present Capabilities and Future Possibilities.
522 *Remote Sensing of Environment*, 35, 243-255.

523 Tucker, C.J., 1979. Red and photographic infrared linear combinations for monitoring
524 vegetation. *Remote Sensing of Environment*, 8, 127-150.

525 Tucker, C.J., Pinzon, J.E., Brown, M.E., Slayback, D.A., Pak, E.W., Mahoney, R., Vermote,
526 E.F., El Saleous, N., 2005. An extended AVHRR 8-km NDVI dataset compatible
527 with MODIS and SPOT vegetation NDVI data. *International Journal of Remote
528 Sensing*, 26, 4485-4498.

529 Turcotte, K.M., Lulla, K., Venugopal, G., 1993. Mapping Small-scale Vegetation Changes
530 of Mexico. *Geocarto International*, 8, 73 - 85.

531 Weiss, J.L., Gutzler, D.S., Coonrod, J.E.A., Dahm, C.N., 2004. Long-term vegetation
532 monitoring with NDVI in a diverse semi-arid setting, central New Mexico, USA.
533 *Journal of Arid Environments*, 58, 249-272.

534
535

Research highlights

- Long term satellite imagery revealed vegetation dynamics of the Australian arid zone.
- Total vegetation response, seasonality and episodic events were the main factors of variability.
- A new zonation was created through unsupervised classification of the main factors of variability.
- Investigation of this new zonation increased understanding of arid zone vegetation dynamics

Figure 1

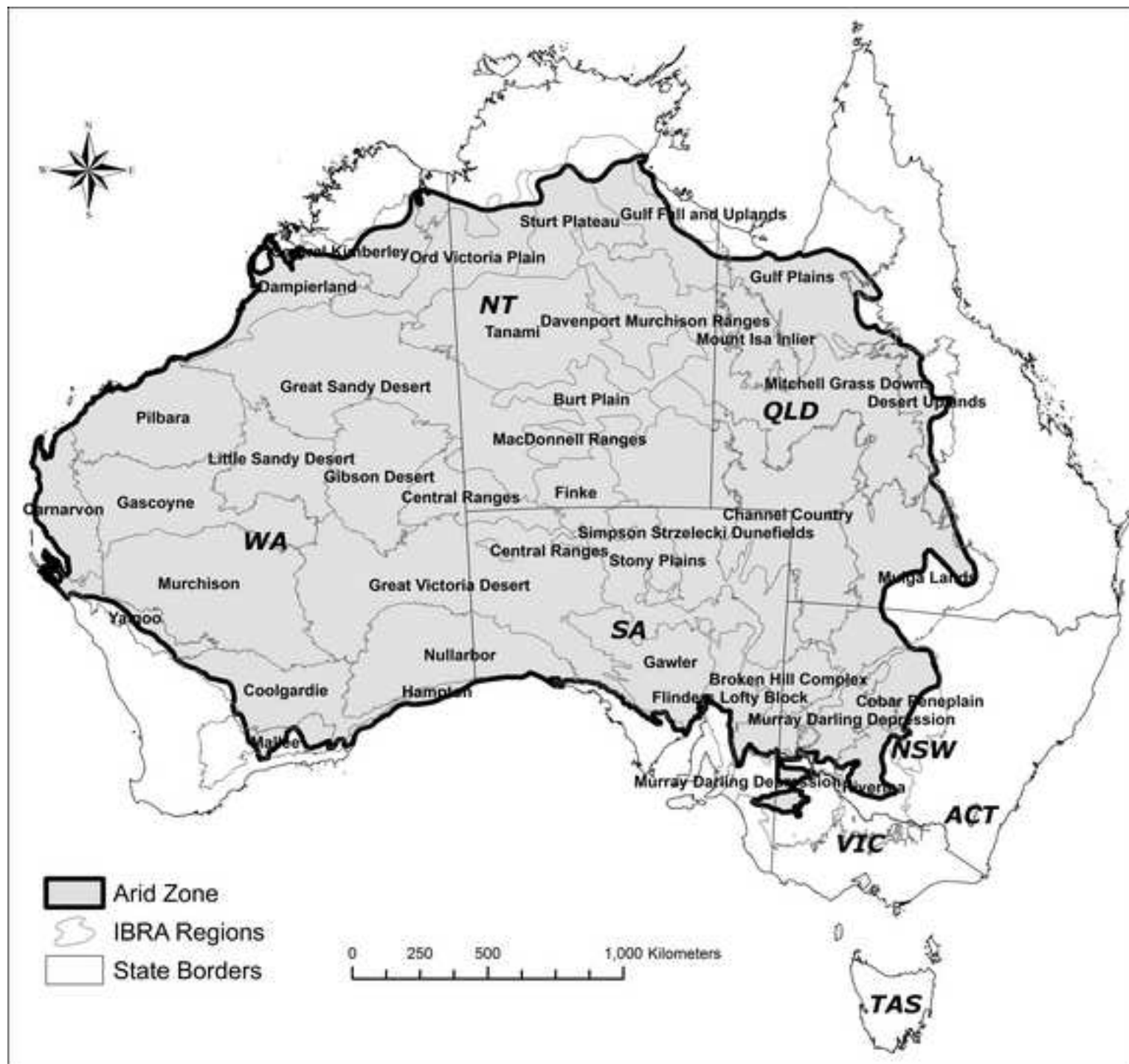


Figure 2

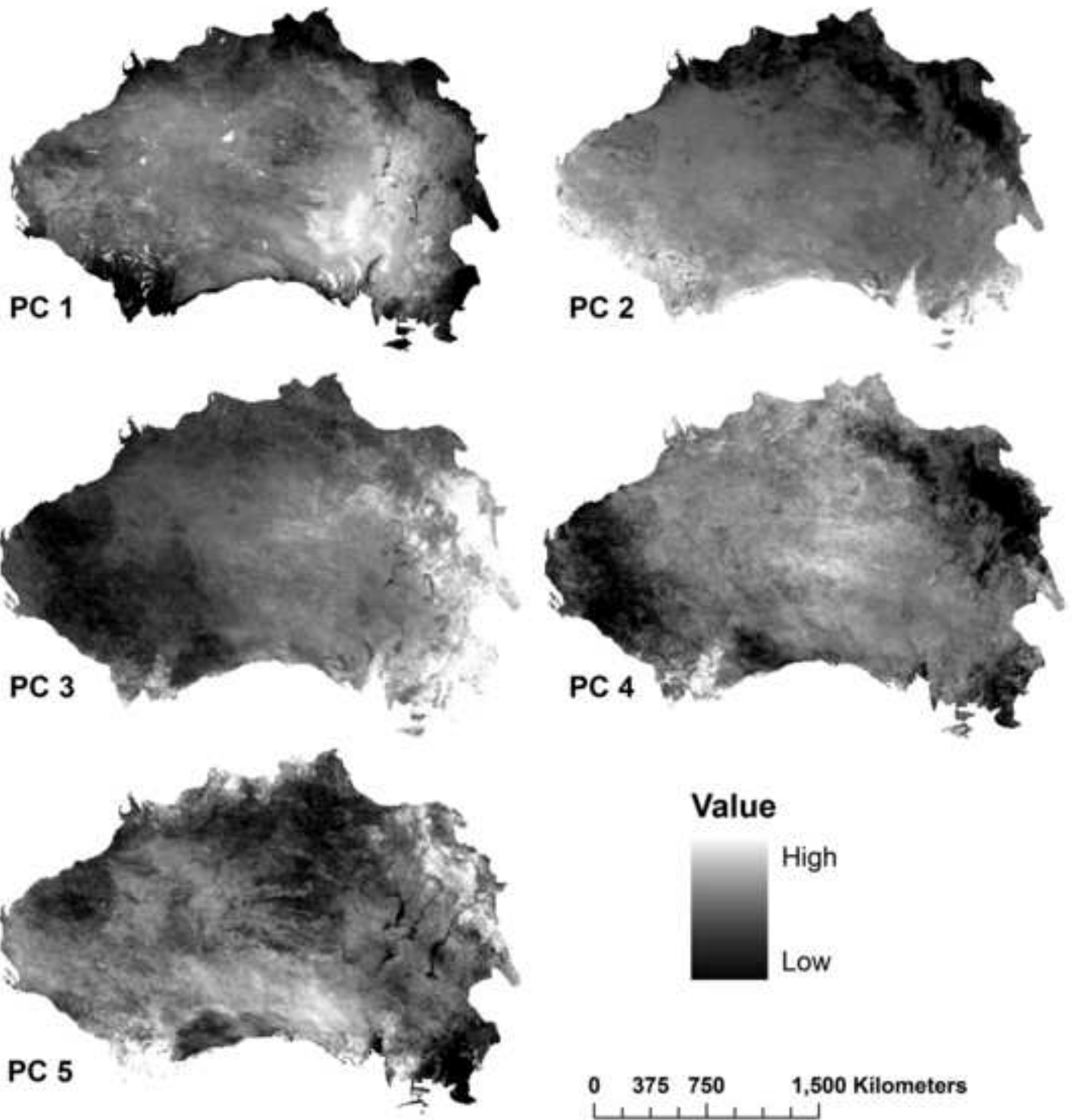


Figure 3

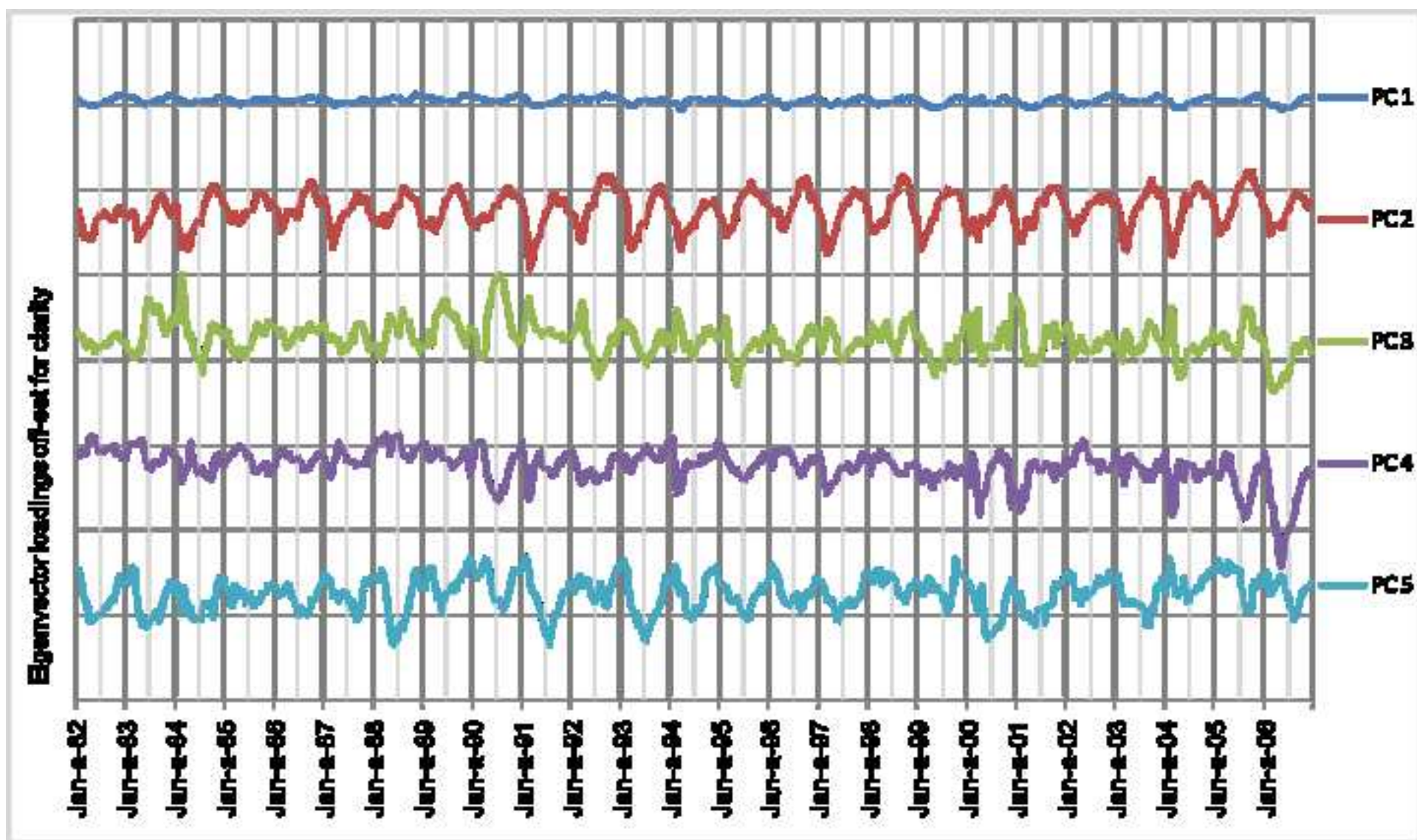


Figure 4

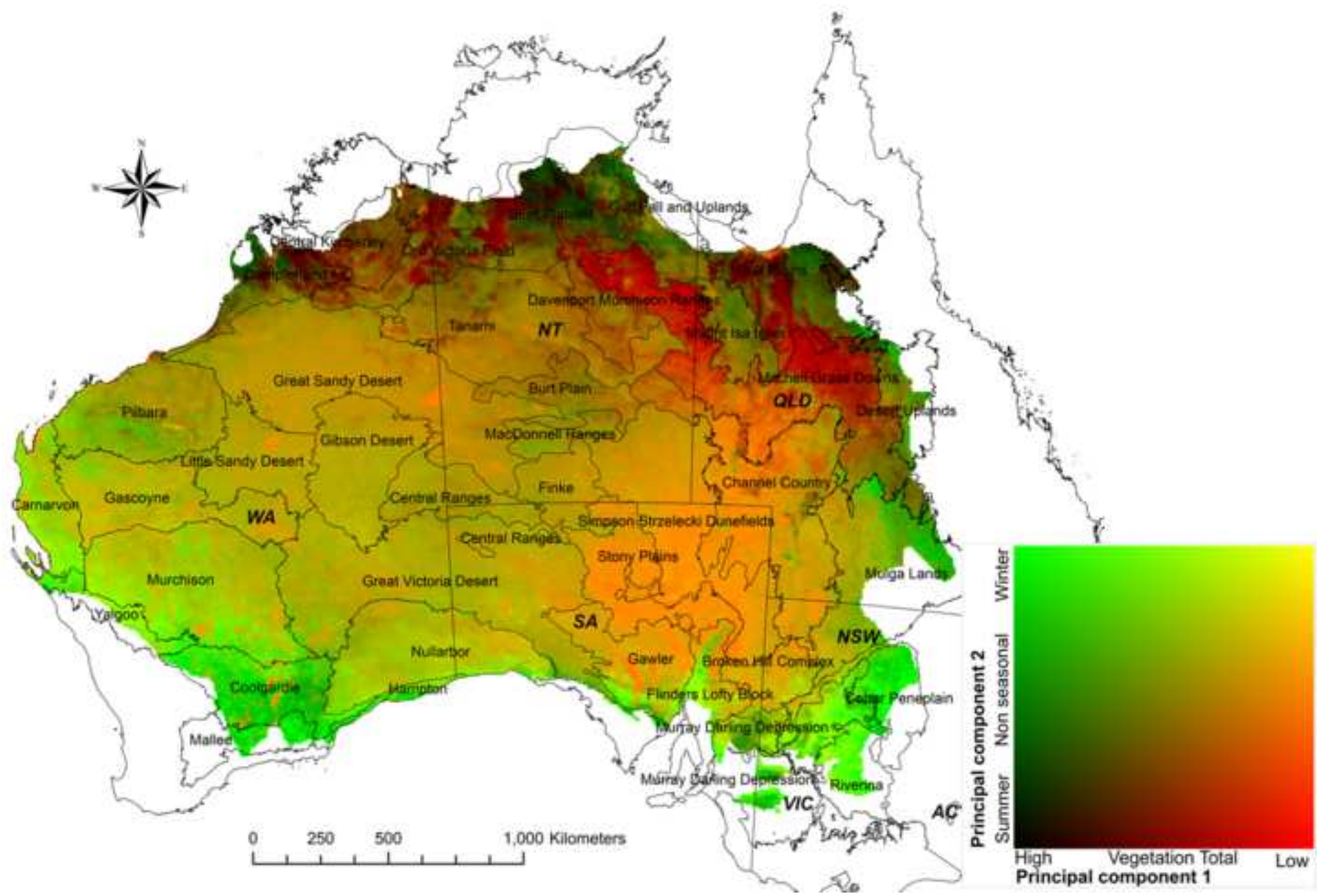


Figure 5

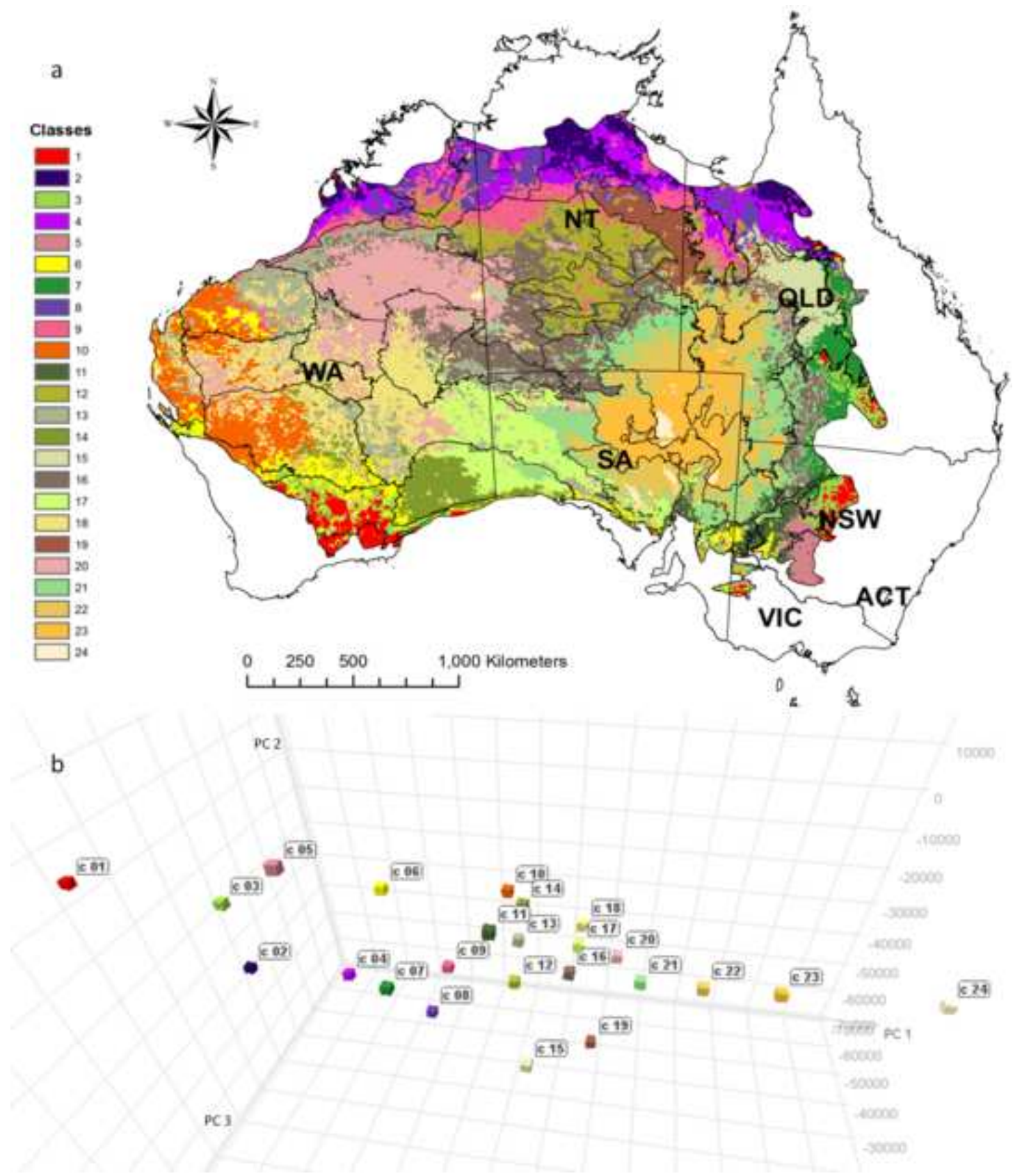


Figure 6

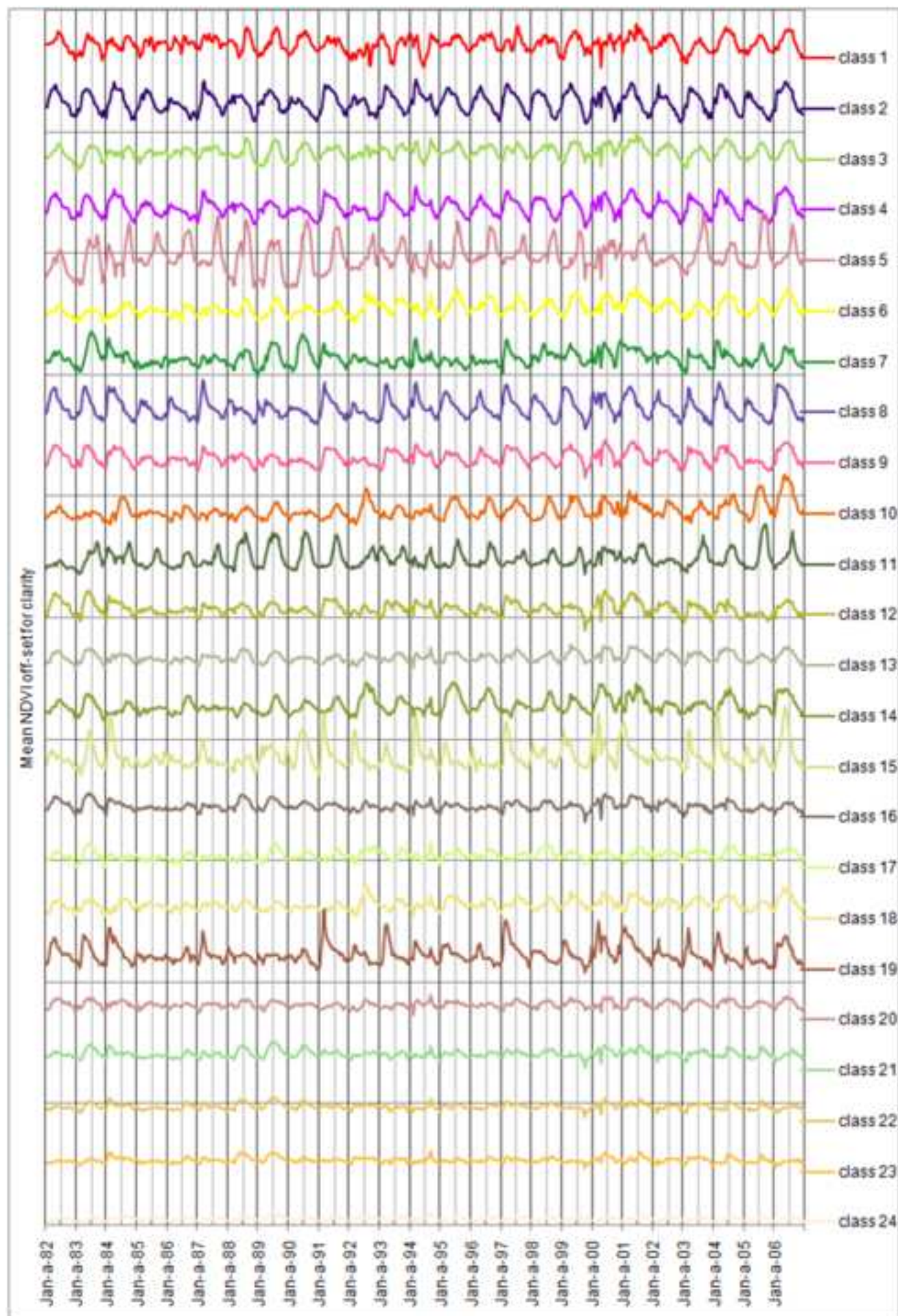


Figure 1. The study area comprising the Australian arid zone excluding cultivated areas. Biogeographical regions defined by IBRA vs 6.1 are shown.

Figure 2. Principal components 1 to 5.

Figure 3. Plot of eigenvector band loadings of the first 5 principal components

Figure. 4. Colour composite of PC1 (red) and PC2 (green) with IBRA regions overlaid to indicate approximate locations. Legend block shows colour interpretation.

Figure 5. a. Geographic distribution of 24 classes resulting from unsupervised classification of the first 14 PCs of 25 year NDVI, with overlay of IBRA vs 6.1 regions; b. 3-D plot of class scores for PC 1, 2 and 3.

Figure 6. The variation in NDVI response over 25 years for each class.

Table 1. Percentage of variance captured by some of the 600 principal components.

Table 2. IBRA regions in the arid zone showing percentage of IBRA occupied by each class.

Table 1. The percentage of variance captured by several of the 600 principal components.

	<i>PC 1</i>	<i>PC 2</i>	<i>PC 3</i>	<i>PC 4</i>	<i>PC 5</i>	<i>PC 6</i>	<i>PC 7</i>	<i>PC 14</i>
Percentage of variance	65.05	7.15	2.97	2.10	1.45	1.12	1.05	0.50
Cumulative percentage of variance	65.05	72.20	75.17	77.27	78.72	79.84	80.89	85.37

Table

IBRA region	1	2	3	4	5	6	7	8	9	10	11	12	13	14	15	16	17	18	19	20	21	22	23	24	
Mallee	76	17				6								1											
Coolgardie	35	35				23							1	2				1		1		1			
Cobar Penepn	37	45			11		6				1														
Desert Uplnds	3	1	19	9			52					6	2		4	4									
Sturt Plateau		49		28				4	17			2													
Gulf Fall n Up		19		49				2	28			2													
Gulf Plains	1	16		37				23	5			2			10	1			3			1			
Dampierland	1	17		35				19	22			1	3								1	1		1	
Riverina	1		2		81	2					13														
Central Kimber				17				31	40			11													
Mount Isa Inlr				17				2	41			20	5		1	6				5	1	1			
Ord Vict Plain		1		17				43	26			12													
Yalgoo	1		16			40				39	1								1		1			1	
Murchison			1			13				34			5	10					31		5	1	1		
Carnarvon						9				50			11						18		6	2	2	2	
Pilbara						10			6	29			38			1			13		2		1		
Murray Darl Dn	5		17	1	18	15	2				34		2				4					3			
Darling Riverin			1			2	4				52	1	1			10	2					24	1	1	2
Davenport Mu								1	13			73				10				2					
Tanami									18			42	1			31					7	1			
Burt Plain									7			66				25						1			
MacDonnell Rg							6	4				53	4			33						1			
Hampton	14		11			20					1					54									
Nullarbor			1			5							2	47				34	4		2	5	1		
Finke												2	5			71					3	18	1		
Central Ranges												21				66	7	1			4	1			
Grt Victoria Ds					3							15	2		3	38	18				9	9	3		
Mitchell GrsDn				1			11	3	2			3	1		28	4				29	1	5	10	3	
Little Sandy Ds												14				4			31		49		1	1	1
Gascoyne						1				16		7	1						49		23		3		
Gibson Desert												3				17	4	36	38		38	1			
Great Sandy Ds								2				2	12			23		1		56		2	1	1	1
Mulga Lands	4		15				23				3	1	14			22						15	2		
Flinders Lfty B			1		3	5					21		2			1	6					29	19	12	
Gawler			2			4					5	3				14					1	15	39	11	6
Channel Cntry						1						2	2			12				2	2	28	27	23	
Broken Hill Cm						1					14					2	1					45	35	3	
Simpson Strzel												1				9						21	36	29	5
Stony Plains																1					1	10	24	63	1